PCCP

The influence of phosphorothioate on charge migration in single and double stranded DNA. A theoretical approach.

Journal:	*Physical Chemistry Chemical Physics*
Manuscript ID:	CP-ART-03-2015-001382.R2
Article Type:	Paper
Date Submitted by the Author:	13-Jul-2015
Complete List of Authors:	Karwowski, Boleslaw; Medical University, Food Science

Journal Name

RSCPublishing

ARTICLE

The influence of phosphorothioate on charge migration in single and double stranded DNA. A theoretical approach.

Cite this: DOI: 10.1039/x0xx00000x

Received ooth January 2012,
Accepted ooth January 2012

DOI: 10.1039/x0xx00000x

www.rsc.org/

B.T. Karwowski[a]

In this study the influence of the phosphorothioate internucleotide bond on the electronic properties of single and double-stranded short nucleotides was investigated at the M06-2X/6-31+G** level of theory in the gaseous phase. Due to the chirality of the phosphorus atom in a phosphorothioate (PT) internucleotide diester bond, the adiabatic/vertical mode of electron affinity/ionization potential, spin density and molecular orbital distribution, as well as structural analysis, were taken under consideration for the single stranded (*ss*) R_P and S_P diastereomers of d[G_{PS}G] and for double stranded (*ds*) d[G_{PS}G]*d[C_{PO}C], in comparison with the corresponding parent phosphate compounds. Moreover, the excitation states, HOMO and LUMO energies were calculated using a TD-DFT methodology at the M06-2X/6-31+G**//M06-2X/6-31++G** level of theory in the aqueous phase. The obtained results show that the PT plays a significant role in the case of *ss*-oligonucleotides, and to a much smaller extent in *ds*-oligomers.

Introduction

In 1988, during the agarose gel electrophoresis of *Streptomyces lividans* DNA, Zhuo *et al.* found a strange DNA degradation phenomenon **[1]**. For many years, the structure and chemical nature of the observed modified compounds had been unclear, mostly due to their low abundance, instability, and purification problems. **[2]**. Nineteen years later, Wang et al. defined it as phosphorothioate (PS) internucleotide linkages **[3]**. The incorporation of sulfur into the DNA sugar-phosphate backbone was assigned as a stereo-specific and sequence dependent process, in which the phosphorus atom within d[G_{PS}G], and d[G_{PS}A] motifs adopts the R_P configuration (**Figure 1**) **[3]**. (The replacement of one of the non-bridging oxygen atoms in the internucleotide phosphodiester bond with sulfur leads to a new P-chiral centre). Following Eckstein's works, Kole proposed that phosphorothioate oligodeoxyribonucleotides (PS-Oligo) can be useful as an RNaze-H activators **[4, 5]**. This strategy is known as one of the antisense mechanisms **[6]**. Moreover, Eckstein showed that using the *Escherichia coli* DNA-dependent RNA-polymerase and [S_P]-NTPαS as substrates, the synthesis of all-[R_P]-PS-RNA oligonucleotides is possible. These studies were extended with synthesis of all-[R_P]-PS-DNA using Polymerase I isolated from *E.coli* **[7]**. Over the next decades, the PS-Oligo have been intensively investigated **[8]**. For chemical synthesis of P-stereodefined PS-Oligo Stec developed the oxathiaphospholane strategy **[9]** although a few other metohods have been proposed recently [**10**]. For many purposes also P-stereorandomal PS-Oligo were tested. In 1998, P-stereorandomal phosphorothioate 21-mer was approved by the FDA (Food and Drug Administration) as a drug - Fomivirsen **[11]**. Although the position of PS-Oligo as potential therapeutic agents or molecular probes is unquestionable, the role(s) of phosphorothioate modification in the bacterial genome is still obscure. Wang and Deng have postulated that the phosphorothioate bond can play an antioxidand/protection role **[12]**. Because genetic information is continuously exposed to

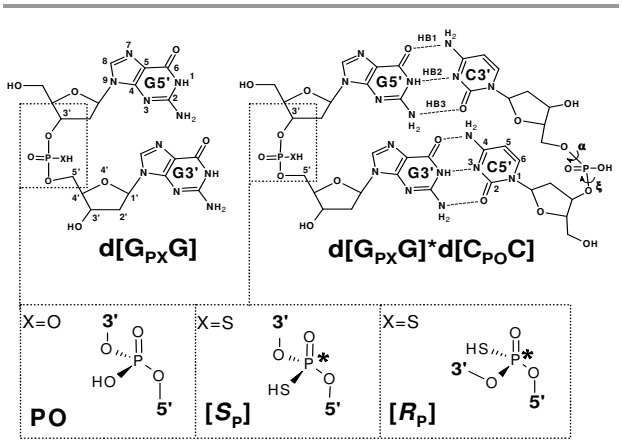

Figure 1. Graphical representation of d[G_{PX}G], d[G_{PX}G]*d[C_{PO}C] structures, phosphorothioate internucleotide bond stereochemistry, hydrogen bonds indication (HB1: O6-N4, HB2: N1-N3, HB3: N2-O2 and diagnostic dihedral angels: O3'-P-O5'-C5' (α), C3'-O3'-P-O5'(ξ), which have been taken under theoretical consideration.

oxidative stress, which can lead to a variety of DNA lesions, simple systems for its protection are beneficial for bacteria **[13]**. On the other hand, under strong oxidative condition phosphorothioate diester bonds in PS-Oligos can be converted to phosphates **[12]**. In this article the influence of the sulfur atom in the sugar-phosphate backbone on charge migration through model double or single-stranded DNA was taken under theoretical consideration.

Results and discussion

It is well established that amongst all nucleobases 2'-deoxyguanosine (dG) possesses the lowest ionization potential. Thus, dG can be easily converted to 8-oxo-2'-deoxyguanosine (8-oxo-dG), which is the most common DNA lesion **[14]**. Therefore, in this study a model dinucleotide d[G_{PX}G] (X=O or S) and a simple duplex d[G_{PX}G]*d[C_{PO}C] were used (**Figure 1**). In 2006, Schuster demonstrated that spermine disulfide can protect *ds*-DNA against oxidative damage **[15].** Wang *et al.* have postulated that phosphorothioate diesters can act as an antioxidant **[12].** Next, Wu observed the desulfurization process, induced by a hydroxyl radical during electrospray ionization mass spectroscopy in a negative mode **[16]**. One-electron oxidation of DNA containing the PT moiety was investigated for the first time by Sevilla *et al.* **[17]**. The authors claimed that the backbone-to-base hole-transfer mechanism was induced by an anionic radical $Cl_2^{\bullet-}$. This process can lead to the formation of either a nucleobase radical cation or a disulfide bond between two adjacent phosphorothioate internucleotide bonds (on the intra or intermolecular path). Because the red-ox potential of the P-S$^{\bullet}$Cl moiety is higher than that of guanine, but lower than for the remaining nucleobases, only one-electron oxidation of Gua is induced. From another point of view, the modification of nucleotides can occur during the electron/radical transfer through double-stranded DNA (*ds*-DNA). Hypothetically, different diastereomeric forms of phosphorothioate internucleotide bonds (of [R_P] or [S_P] absolute configuration) can influence charge migration and successfully protect some of the remaining DNA parts against degradation. The type and "quality" of these changes in the single-stranded and double-helix DNA chains should depend on the phosphorus atom configuration i.e, S_P or R_P.

The initial geometries of the investigated nucleotides were taken from a 2R8J.pdb structure **[18]** and converted into suitable d[G_{PO}G], d[G_{PO}G]*d[C_{PO}C], [R_P]/[S_P] d[G_{PS}G] and [R_P]/[S_P] d[G_{PS}G]*d[C_{PO}C] structures (**Figure 1**). The obtained molecules were fully optimized at the M06-2X/6-31+G** level of theory in the gaseous phase. In all cases, the B form of DNA was observed. Local base and base-pair step parameters were assigned accordingly to the oligonucleotides standard reference frame analysis **[19]**.

Neutral Form

The results of analyses show little structural differences between neutral forms of the investigated phosphate and thiophosphate oligonucleotides (**Table 1**). It is particularly seen for a *Rise* parameter, which "determinates" the energies of stacking interaction. For *ss*-DNA, the differences between d[G_{PO}G] and [R_P] and [S_P] d[G_{PS}G] were 0.19Å and 0.08Å, respectively. For *ds*DNA, the fluctuation of the *Rise* value did not exceed 0.01Å. Also *Shift*, *Slide*, *Tilt*, *Roll*, and *Twist* parameters did not differ significantly (**Table 1**, **Figure 1SM;** supplementary material, **SM**). However, in the case of d[G_{PX}G] (X=O or S) analogues, due to the lack of hydrogen bonds and unrestricted flexibility, the discussed divergences were higher than for d[G_{PX}G]*d[C_{PO}C]. Moreover, the sulphur atom in the internucleotide bond gives rise to a slight elongation of the hydrogen bond (**Table 1SM**). The geometries of sugar phosphate backbones, determined by the dihedral angles: O3'-P-O5'-C5' (α) and C3'-O3' -P-O5' (ξ), are moderately upset in d[G_{PX}G] systems (**Table 1SM**). This influence of the PT was less pronounced in d[G_{PX}G]*d[C_{PO}C] molecules, as the observed α and ξ angle fluctuations were at the level of 5.1°, except for α=41.2° for R_P isomer of the d[G_{PS}G] strand in the duplex (**Table 1SM**).

Table 1. Local base and base-pair step parameters of d[G_{PX}G] and d[G_{PX}G]*d[C_{PO}C] (X=O or S) calculated by W3DNA software

System	Local base and base-pair step parameters					
	Shift [Å]	*Slide* [Å]	*Rise* [Å]	*Tilt* [°]	*Roll* [°]	*Twist* [°]
d[G_{PX}G]						
CATION						
PO (X=O)	-1.68	-0.79	2.90	-10.98	2.40	-61.49
[S_P] (X=S)	0.69	-0.42	3.12	4.51	-0.77	-40.74
[R_P] (X=S)	0.81	-0.46	3.22	6.68	0.09	-42.52
NEUTRAL						
PO (X=O)	-1.49	-0.03	3.01	-1.10	1.34	-57.23
[S_P] (X=S)	-1.71	-0.40	2.93	-6.70	2.29	-61.14
[R_P] (X=S)	-1.64	-0.48	2.88	-9.4	1.37	-59.84
ANION						
PO (X=O)	16.61	5.55	10.40	0.65	-10.39	96.75
[S_P] (X=S)	-2.14	-1.14	2.89	-24.54	5.41	-65.30
[R_P] (X=S)	1.98	2.98	4.19	7.66	21.22	-26.27
d[G_{PX}G]*d[C_{PO}C]						
CATION						
PO (X=O)	-0.11	-2.07	3.21	-2.90	7.26	51.40
[S_P] (X=S)	-0.02	-2.04	3.26	-3.64	7.33	51.85
[R_P] (X=S)	-0.52	-1.82	3.25	-4.99	8.41	52.97
NEUTRAL						
PO (X=O)	-0.33	-1.87	3.37	-0.94	7.87	49.54
[S_P] (X=S)	-0.34	-1.87	3.37	-1.07	7.82	49.65
[R_P] (X=S)	-0.43	-1.94	3.38	-1.65	8.91	50.95
ANION						
PO (X=O)	-1.23	-1.86	3.56	-1.25	4.78	44.57
[S_P] (X=S)	-0.91	-1.89	3.77	-1.79	3.76	46.18
[R_P] (X=S)	-1.64	-1.96	3.51	-6.25	7.96	44.90
Reference Parameters						
PO (X=O) ref **[19a]**	-0.02	0.23	3.32	-0.1	0.6	36.50
PO (X=O) ref. **[19b]**	0.4 ±0.31	-1.13 ±0.64	3.57 ±0.31	2.1 ±4.2	2.8 ±5.6	31.4 ±4.5
[R_P] (X=S) ref. **[19b]**	-0.03 ±0.65	-1.18 ±0.82	3.6 ±0.35	0.3 ±4.3	5.2 ±5.3	31.6 ±5.1

Radical Cation Form

When a single electron is removed from a neutral molecule a cation radical is formed. If this process takes place in d[G_{PO}G] (*ss*-DNA), it gets manifested in the 3D geometry with the *Rise* parameter decreasing by 0.11Å. Surprisingly, *Rise* increases for

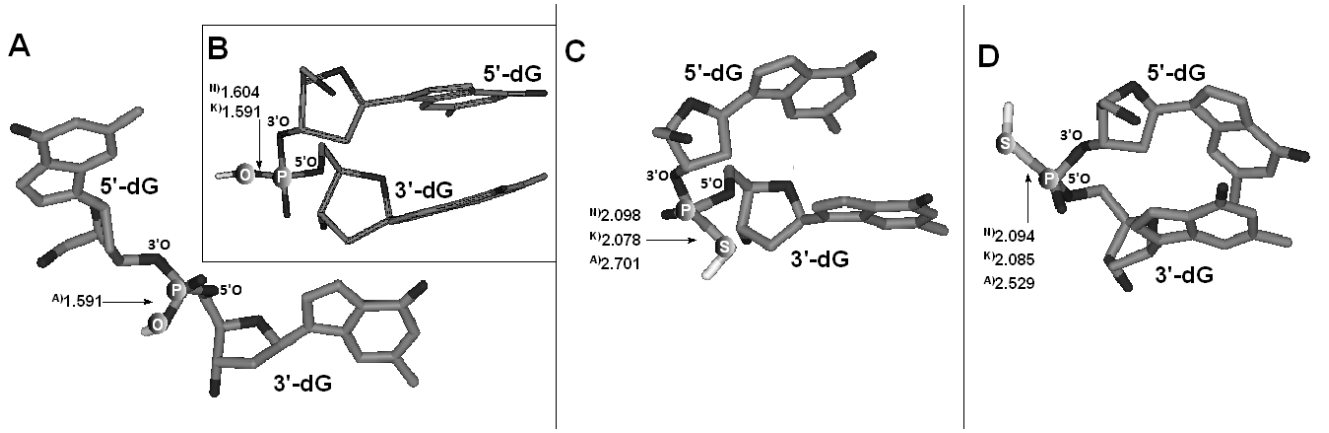

Figure 2. Visualisation of 3-dimensional geometries of optimized structures: Radical anion forms of: A) d[G_{PO}G]; C) [S_P] d[G_{PS}G], D) [R_P] d[G_{PS}G] and B) Radical cation form of d[G_{PO}G]. Length of P-OH and P-SH bond in Neurtral (N), Cation (K) and Anion (A) radical forms are given in Å.

[S_P] and [R_P] diastereomers of d[G_{PS}G] by 0.19Å and 0.34Å, respectively (**Table 1**). Simultaneously: *Shift*, *Slide* and *Roll* parameters showed only negligible fluctuation, independently of the presence or absence of the sulfur atom in the internucleotide linkage. However, *Tilt* for d[G_{PO}G] changed by -9.88°, and increase of *Tilt* and *Twist* for S_P and R_P d[G_{PS}G] by 11,21°, 16,8° and 20.4°, 17.32°, respectively, was observed (**Table 1**). Visualization comparing the spatial geometries d[G_{PO}G] and [S_P]/[R_P] d[G_{PS}G] (presented in **Figure 2SM**) shows that the general shape of the analyzed dinucleotides is quite similar. The ionization related changes of the parameters are less diverse in *ds*-DNA. For all investigated molecules (denoted as d[G_{PX}G]*d[C_{PO}C], X=O or S) the *Rise* parameter value decreased by 0.16Å PO, 0.11Å [S_P], or 0.13Å [R_P]. Other base-pair step parameters demonstrated only negligible fluctuation (**Table 1**). This situation results from the hydrogen bonds (HB) present in the systems, which "stabilize" the stacking interaction in the helix structure. The rigidity of the base pair system was compensated by flexibility of the sugar-phosphate backbone.

Both diagnostic dihedral angles O3'-P-O5'-C5' (α) and C3'-O3'-P-O5' (ξ) of cation radical forms showed the following differences with the corresponding neutral species (**Table 1SM**):

a) for [S_P] d[G_{PS}G]*d[C_{PO}C]: 18.42° and 93.18° on the phosphorothioate strand; 8.81° and 6.1°, respectively, in the complementary unmodified strand

b) for PO and R_P *ds*-DNA molecules: 6.86° for α and 12.45° for ξ in both strands.

Importantly, in all investigated cases the ionization left the pyrimidine strands almost unaffected. As shown in **Table 1SM**, after ejection of the electron from the d[G_{PX}G]*d[C_{PO}C] (X=O or S) systems, the following changes in length of hydrogen bonds were observed:

a) shortened **N1---N3** and **N2---O2** and increased length of **O6--N4** in the $^{5'}$**G:::C**$^{3'}$ base pair,

b) shortened **N1---N3** and increased length of **O6---N4** and **N2---O2** in the $^{3'}$**G:::C**$^{5'}$ base pair .

However, the discussed changes were more intense in the $^{3'}$**G:::C**$^{5'}$ base pair than in the $^{5'}$**G:::C**$^{3'}$ counterpart (**Table 2SM**).

Anion Radical Form

Acquisition of a single electron by d[G_{PO}G] or d[G_{PS}G] leads to the formation of anion radical, with significant structural consequences. As shown in **Table 1**, all the base parameters are completely different from those assigned to the neutral forms. The d[G_{PO}G] anion radical adopts an "open linear form" (**Figure 2A** *versus* **2B**), for which *Roll* and *Twist* of 10.39° and 96.75°, respectively, were found, while the distance between guanine C8 atoms changed from 5.07Å to 10.86Å and the ξ angle increased to 213°. For [S_P] and [R_P] d[G_{PS}G], the base parameters still showed a possibility of stacking interaction (**Figure 2C,D**), with the *Rise* parameter values of 2.89Å and 4.19Å values, respectively. Also, the length of corresponding P-S bonds increased to 2.7Å and 2.53Å and they lost the covalent character. These observations suggested the disparate nature of electron attachment, forced by a lack of a suitable part for its acceptance. A visualized comparison of the spatial geometry of d[G_{PX}G] (X=S or S) radical anion forms is presented in **Figure 3SM**. Addition of the complementary d[C_{PO}C] strand to the investigated systems furnishes (in gaseous phase) duplexes, which are less affected by the extra electron. Thus, the base-pair *Shift*, *Slide*, *Tilt* and *Roll* parameters have values similar (**Table 1**) to those for neutral form of d[G_{PX}G]*d[C_{PO}C] (X=O or S). Also *Twist* decreased only by ~5° (rather uniformly), while for PO, [S_P] and [R_P] forms *Rise* increased by 0.35Å, 0.51Å and 0.26Å, respectively. Within the $^{5'}$**G:::C**$^{3'}$ part in the duplex, the changes in the hydrogen bond length showed the same pattern as for the radical cation forms. For the remaining $^{3'}$**G:::C**$^{5'}$ base pair, a shortened **N1--N3** and elongated **N2--O2** and **O6--N4** bonds were found (**Table 1SM**).

The structural changes resulting from the electron attachment (manifested by change of the *Rise* parameter) affected the conformation of the sugar-phosphate backbone. For both strands of d[G_{PX}G]*d[C_{PO}C], independently of the presence of sulfur in the internucleotide bond, the diagnostic α

and ξ dihedral angles (Table 1SM) deviated from those in the neutral forms. Within the $^{5'}$**G:::C**$^{3'}$ part in the duplex, the changes in the hydrogen bond length showed the same pattern as for the radical cation forms. For the $^{3'}$**G:::C**$^{5'}$ pair decreased **N1--N3** and elongated **N2--O2** and **O6--N4** bonds were found. Contrary to the results obtained for the radical cation forms the changes in hydrogen bond lengths were more intense in the $^{5'}$**G:::C**$^{3'}$ base pair than in $^{3'}$**G:::C**$^{5'}$ (Table 1SM).

Influence of PT Internucleotide Bond on Charge Distributions

For all optimized structures, a charge analysis (summed to heavy atoms) was achieved using Hirshfeld methodology **[20]** at the M062X/6-31+G** level of theory (Table 3SM, 4SM). The charge distribution reveals that in all neutral forms of d[G_{PO}G] and d[G_{PO}G]*d[C_{PO}C] the negative net charge was located mainly on guanine and phosphate groups. Surprisingly, cytosine nucleobases adopted a positive one. These results tally with those on GC–6H_2O **[21]**, in which a large amount of positive charge was found on cytosine. Regardless the stereochemistry of the PT diester bond ([R_P] or [S_P]) the sulfur atom did not change the charge distribution in the investigated structures (Table 3SM, 4SM).

In the radical cations derived from d[G_{PX}G] (X=O, S), in all forms (PO, [R_P] and [S_P]) the positive charge was found on the 5'-end guanine, in almost the same percentage ratio, whereas in the duplexes d[G_{PX}G]*d[C_{PO}C] (X=O or S) the positive charge was mostly located on the 3'-end guanine. Again, neither the presence of sulfur nor the chirality of phosphorus atom affected the charge distribution.

In the radical anions, as expected, the negative charge was mainly located on the 3'-end cytosine. All d[G_{PX}G]*d[C_{PO}C] molecules followed the same distribution scheme for PO, [R_P], [S_P] forms. Importantly, within the d[G_{PX}G]*d[C_{PO}C] neither electron injection nor ejection altered significantly the spatial geometry. However, larger negative charge dispersion was observed for d[G_{PX}G]*d[C_{PO}C] than for d[G_{PX}G] (X=O or S) (Table 3SM, 4SM). Upon transition into the radical cation forms, in both base pairs the length of HB2 and HB3 (**Figure 1**) decreases (Table 1SM, 2SM) and the length of HB1 increases. In the radical anion forms, within the $^{5'}$G:::C$^{3'}$ base pair the length of HB2 and HB3 decreases and that of HB1 increases. For the $^{3'}$G:::C$^{5'}$ base pair, longer HB1 and HB3 and shorter HB2 were found. It should be pointed out, that the electron attachment affects the length of hydrogen bonds in the $^{3'}$G:::C$^{5'}$ more than in $^{5'}$G:::C$^{3'}$. In the case of electron detachment, $^{3'}$G:::C$^{5'}$ is structurally more sensitive than $^{5'}$G:::C$^{3'}$. The calculated differences in HBs distances between neutral compounds and their radical cation or radical anion forms were of 0.258Å and 0.226Å, respectively.

The electron attachment by PO, [R_P], [S_P] forms of single-stranded d[G_{PX}G] (X=O or S) leads to significant structural changes. (The electron affinity for the DNA/RNA bases decreases in the order Ura>Thy>Cyt~Gua>Ade **[22]**.)

In d[G_{PO}G] the negative charge was dispersed over the molecule. Concomitantly, the stacking interactions were disrupted and the structure became linear. Because the negative charge was in 53% located on the 3'-end dG sugar moiety, the dipole moment (DM) increased up to 18.41 D (Table 3SM). For [R_P] and [S_P] diastereoisomers of d[G_{PS}G] the negative charge was mainly located on the thiophosphate unit and the stacking interactions were preserved. Therefore, the general shape of the anionic molecules was similar to their neutral precursors. The corresponding differences in dipole moments for [R_P] and [S_P] diastereoisomers (calculated as $DM_{Radical\_Anion}$—$DM_{Neutral}$) were 3.51 D and 3.33 D, respectively. Simultaneously, the P-S bonds got longer by 0.6Å and 0.44Å respectively, so they adopted a more "radical" ionic character, rather than covalent. Also, the O5'-P bonds in [R_P] and [S_P] d[G_{PS}G] lengthened by 0.078Å and 0.109Å, respectively, compared to 0.018 Å for d[G_{PO}G]. The above observations are in good agreement with Leszczynski's studies on near-zero-electron volt electron attachment **[23]**. Importantly, in the dinucleotides the N-glycosidic bonds (C1'-N9) and O3'-P bonds are less affected by electron detachment or attachment. In double-stranded forms (either neutral or radical anion/cation), the elongation of O5'-P bonds in both strands were virtually negligible (Table 4SM). The same was observed for other bonds important for genome stability and integrity, i.e. C1'-N9, C1'-N1 and O3'-P (Table 4SM). However, in each duplex the scant elongation of the mentioned linkages in the d[G_{PX}G] (X=O or S) strand in a radical cation form was denoted. For all molecules, the highest deviation value of 0.034Å was assigned for the C1'-N9 bond in 3'-end dG of [R_P] d[G_{PS}G]*d[C_{PO}C]. For the d[C_{PO}C] strand, in the radical anion mode, a slight shortening of the C1'-N1 linkage by 0.028Å, 0.03Å, 0.03Å were noted in 3'-end dC for [S_P], PO and [R_P] forms of d[G_{PX}G]*d[C_{PO}C] (X=O Or S), respectively, compared to the neutral forms.

The assigned scheme of selected bond elongations and shortenings are in good agreement with the calculated charge distribution over the discussed molecules.

For the radical cation/anion forms, where the positive/negative charge is mainly localized on the $^{3'}$G:::C$^{5'}$/$^{5'}$G:::C$^{3'}$, the length of HB2 decreases, HB1 increases with subsequent scant HB3 fluctuation were noted (Table 2SM), in comparison with suitable neutral forms. The observed changes of corresponding hydrogen bond lengths in the "complementary" stacked base pair were negligible (Table 2SM).

Spin Density and Molecular Orbital Localisation

Much theoretical (DFT) work has been done on electronic structures of stacked nucleoside bases or base pairs (without taking into account a sugar-phosphate backbone), as models of single or double-stranded DNA **[**e.g. **21-24]**. Only few of published papers deal with mononucleotides or dinucleotides. No data is available for *ds*-DNAs (even short) and their [R_P] or [S_P] phosphorothioate analogs.

Molecular Orbital Localisation

The set of performed calculations showed that in d[G_{PO}G], and [R_P] and [S_P] d[G_{PS}G] systems the highest occupied molecular

orbital (HOMO) is localized on the 5'-end guanine heterocycle (**Figure 4SM**). On the contrary, in the double-stranded PO and S_P d[G_{PX}G]*d[C_{PO}C], HOMO was diffused over the 3'-end guanine moiety of $^{3'}$G:::C$^{5'}$ base pair (**Figure 5SM**), while in [R_P] d[G_{PS}G]*d[C_{PO}C] HOMO was distributed also on the guanine belonging to the $^{5'}$G:::C$^{3'}$ part (**Figure 5SM**). To explain these facts one can take into account that in the [R_P] diastereomer the double-helix structure is much disturbed due to steric interaction with the H2' of the proximal nucleoid **[25]**, and the molecular orbitals and spin density are strongly structure dependent **[26]**. It must be emphasized that for d[G_{PO}G]*d[C_{PO}C] and [S_P] d[G_{PS}G]*d[C_{PO}C], *Tip* values of 1.64, 2.27, and *Inclination* values of 6.29, 4.78, respectively, were found, while those for [R_P] d[G_{PS}G]*d[C_{PO}C] were distinctly different (8.06 and 10.27, respectively). Thus, the diffusion of HOMO is not surprising.

Figures 4SM and **5SM** show the lowest unoccupied molecular orbitals (LUMO) plotted for all investigated molecules. For d[G_{PX}G]*d[C_{PO}C] (X=O or S) LUMO was localized on the pyrimidine strand. As concluded in previous works **[23,27],** the lowest unoccupied molecular orbital was found around the sugar-phosphate backbone. The same LUMO distribution was found in the single strand d[G_{PO}G] and [S_P] d[G_{PS}G] (**Figure 4SM**). Surprisingly, in the case of [R_P] d[G_{PS}G], LUMO was dispersed also over the bases, and actually, the main part of LUMO has been found around the stacked guanines (**Figure 5SM**). The described above differences indicate a crucial role of the position of the sulfur atom for the HOMO/LUMO distribution.

SPIN DISTRIBUTION

One electron oxidation/reduction processes constitute a typical initial step for DNA damage. Ionizing radiation applied to a cell, which contains 80% of water, may lead to radiolysis of water molecules and formation of reactive oxygen species (ROS). As the result, remarkable amounts of electrons are released. ROS and solvated electrons can interact with DNA, causing their damage (an indirect route). The damage can be done also on a direct route during interaction of the radiation with an oligonucleotide, resulting in electron ejection (formation of a radical cation), or electron attachment (formation of a radical anion). Sevilla *et al.* have shown, that during γ-radiation of oligonucleotide the radicals are formed in the following amounts: 35% Gua●+, 5% Ade●+, and about 45% of Thy●- and Cyt●- **[28]**. The charge may migrate along a DNA chain through a single-step tunneling or multistep hopping (random-walk or polaron-like). For all mechanisms the charge migration strongly depends on structural factors as hydrogen bonds, base pairs stacking, etc. A "hole" (the place with a positive charge and spin localization, produced by electron loss from the molecule) can migrate through DNA, until is trapped by an appropriate system, usually a Gua-reach oligonucleotide segment. This is because guanine has the lowest ionization potential and is the easiest moiety to get oxidized. Sugiyama and Saito demonstrated that ionization energy decreases with an increasing number of consecutive guanosines (7.75, 7.28, 7.07, and 6.98 eV for Gua, Gua2, Gua3, and Gua4, respectively) **[29]**. In oligonucleotides, the hole can jump from one nucleic base to another, finally localizing at the 5'-end Gua in a guanosine rich part of the strand **[26,30]**. Therefore, the charge and spin should be observed there.

In accordance with previous studies **[26,29]**, the adiabatic radical cation in d[G_{PO}G] has been found almost exclusively on the 5'-end Gua. In the case of [R_P] and [S_P] d[G_{PS}G], the "hole" is mainly present on 5'-end G, with scant dispersion on the 3'-end guanine (**Figure 6SM**). It should be pointed out that in the phosphorothioate analogs the nucleobase rings overlapping is altered (Twist changed from 61.49° to 40.74° or 42.52°, **Table 1**, **Figure 2SM**). In relaxed radical cation forms, the spin density calculated on the atoms within the 5'-end Gua decreased in the order C8>C5>N3>O6>C4>N2 (values higher than 0.09 are noted), independently of the nature of an internucleotide bond (**Figure 7aSM**). In corresponding vertical radical cation forms, the highest spin was found on the C5 atom; secondly, a higher value was observed on O6 than on the C4 atom, although the unrelaxed structures of the neutral forms were taken into calculation.

For double-strand d[G_{PX}G]*d[C_{PO}C] (X=O or S) radical cations, the positive charge and spin were found on Gua belonging to the 3'G:::G5' base pair. However, contrary to [S_P] d[G_{PS}G]*d[C_{PO}C] and d[G_{PO}G]*d[C_{PO}C], where the spin was exclusively localized on 3'-Gua, in the [R_P] counterpart a partial dispersion of the spin on Gua in the 5'G:::C3' base pair was noticed (**Figure 8SM**). The spin density distribution in the 3'G:::C5' pair in d[G_{PX}G]*d[C_{PO}C] (X=O or S), for radical cation forms (depicted in **Figure 7bSM**), decreases in the following order: adiabatic, PO, [S_P], [RP], C5>C8>N3>N2>O6; vertical, PO and [S_P], C5>N3>C8>N2>O6; [R_P], C5>N3>C8>O6>N2. These patterns are in good agreement with the highest occupied molecular orbital localization in the parent neutral form of the discussed double-stranded models (**Figure 5SM**).

The similarity of the assigned local base-pair step parameters and the 3D geometry of d[G_{PX}G]*[C_{PO}C] (X=O or S) (**Table 1**, **Figure 8SM**) suggests that the sulfur atom in the internucleotide bond of [R_P] configuration is important for the hole migration process through *ds*-DNA.

The electron capture by a molecule leads to the radical anion formation, and in a dG reached part of *ss*-DNA it is strongly clustering level dependent **[31]**. The analysis of the lowest unoccupied molecular orbital (LUMO) in d[G_{PO}G] and [S_P] d[G_{PS}G] showed its localization near the sugar-phosphate moiety (**Figure 4SM**). Unexpectedly, for [R_P] d[G_{PS}G] LUMO was mainly localized on the side of stacked guanines and very little, if any, on the phosphorothioate part. These observations suggest different consequences of electron abatement

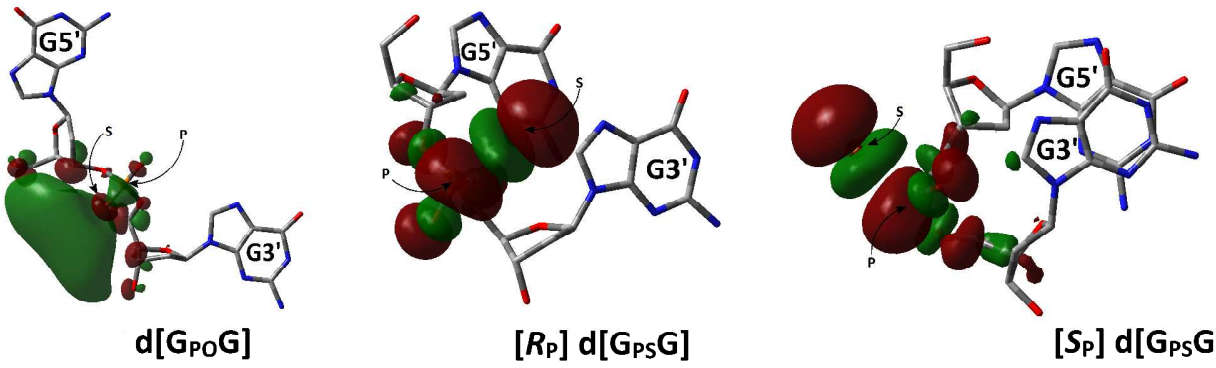

Figure 3. The SOMO of radical anion forms of **d[G_{PO}G]**, **[S_P] d[G_{PS}G]** and **[R_P] d[G_{PS}G]**, calculated at M06-2X/6-31+G** level of theory. **G3'**–3'-end guanine, **G5'**–5'-end guanine.

As to the geometry, the formation of a radical anion by d[G_{PO}G] leads to structure linearization and spin localization exclusively next to the sugar-phosphate backbone. Moreover, in dG5' elongation of the bonds O5'-P, O3'-P and C1'-N9 by 0.018Å, 0.025Å and 0.19Å, respectively, was observed, with the length of the C1'-N9 bond on dG3' remaining unchanged (**Table 3SM**, **Figure 2**). For [S_P] and [R_P] d[G_{PS}G] the influence of an excess electron on the geometry is less visible. However, the spin localization on the sulfur and phosphorus atoms leads to elongation of the P-S bonds by 0.612Å and 0.435Å, respectively. Because the SOMO analysis showed their antibonding character (**Figures 3** and **9SM**), one can postulate that in [S_P] and [R_P] d[G_{PS}G] the P-S bonds should be broken. Moreover, the mentioned spin localization on this part of molecules leads to the slackening of other important bonds for genome integrity i.e.: O3'-P by 0.094/0.08Å, O5'-P by 0.08/0.11Å, C1'-N9 (5'-end dG) by 0.02/0.06Å for the [S_P]/[R_P] d[G_{PS}G], respectively (**Figure 7aSM**, **Table 3SM**). These observations are in good agreement with results presented by Leszczynski *et al.* for DNA strand brakes induced by near-zero-electron volt electrons **[23].**

The above results may be pertinent to a loss of sulfur observed during negative electrospray ionization mass spectrometry (ESI) experiments done on PS-DNA **[16]**. Wu *et al.* have proposed that the sulfur atom can be replaced by an oxygen atom via a radical mechanism, as shown in **Figure 4A**. On the other hand, it was shown that an H-phosphonate dinucleotide is an intermediate in the desulfuration process (**Figure 4B**) **[12]**. In both cases, attachment of a low energy electron by the phosphorothioate moiety can be an initial step leading to the elongation of the P-S bond.

The situation is different in the case of *ds*-DNA. It is well known that "*Double-stranded DNA does not capture electrons as efficiently as single-stranded oligomers; however, once captured, the electrons are bound more strongly than to the single strands*" **[31]**. Moreover, double stranded DNA is much more rigid and regular than single stranded oligomers (see **Table 1, Figure 10SM**). The analysis of LUMOs revealed no differences between their localization in d[G_{PO}G]*d[C_{PO}C] and d[G_{PS}G]*d[C_{PO}C] (**Figure 5SM**). The electron capture by *ds*-oligonucleotides led to spin localisation exclusively on 3'-dC, independently of the presence of sulfur in the structure. For vertical and adiabatic radical anions of d[G_{PO}G]*d[C_{PO}C], [R_P] and [S_P] d[G_{PS}G]*d[C_{PO}C], spin density decreased in the order C6>C4>N3>N1 (**Figure 7bSM** and **10SM**). Thus it seems that the presence of phosphorothioate linkage does not play any significant role in the electron capture/migration process through *ds*-DNA.

Electronic properties of d[G_{PX}G]*[C_{PO}C] and d[G_{PX}G] (X=O or S)

The electronic properties of nucleic bases, nucleosides and

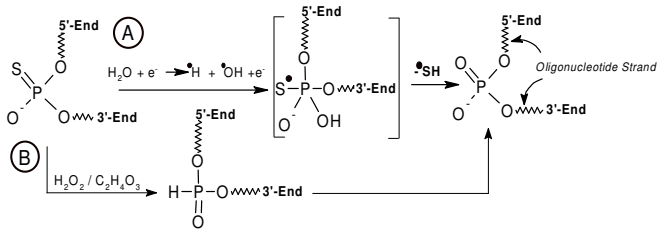

Figure 4. Two possible mechanisms of internucleotide phosphorothioate bond desulfurization.

nucleoside pairs have been studied theoretically and experimentally **[32]**. **Figure 5** and **Table 2** show a relationship between adiabatic/vertical ionization potentials (AIP, VIP), adiabatic/vertical electron affinities (AEA, VEA), vertical electron attachment/detachment energies (VEAE, VEDE), and nuclear relaxation energies (NRE), in single- and double-stranded phosphorothioate DNA analogs.

Ionisation Potential

For the *ss*-DNA models, AIP and VIP are in the range of 0.17eV and decrease in the order: [S_P] d[G_{PS}G]>[R_P] d[G_{PS}G]>d[G_{PO}G]. Surprisingly, the lowest VIP value was found for [S_P] d[G_{PS}G]>d[G_{PO}G]>[R_P] d[G_{PS}G]. However, the differences between VIPs were negligible (<0.07eV, **Table 2**). On the other hand, the highest VEAE, which is responsible for

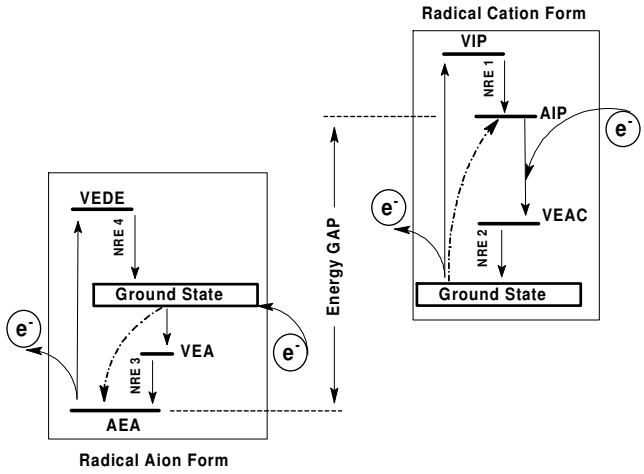

Figure 5. The scheme of energy changes during the electron attachment/detachment process of investigated systems. Details are given in the experimental part.

Table 2. Calculated electronic properties of d[G_{PX}G]*d[C_{PO}C] and d[G_{PX}G] (X=O or S) at M06-2X/6-31+G** level of theory in the gaseous phase and excitation energies as well as HOMO LUMO energies at TD-DFT M06-2X/6-31++G** level of theory in the aqueous phase. Energies are given in eV.

M06-2X/6-31+G** in gaseous phase						
Electronic properties	d[G_{PX}G]			d[G_{PX}G]*[C_{PO}C]		
	X=O	X=S		X=O	X=S	
		[R_P]	[S_P]		[S_P]	[R_P]
IP	6.93	7.05	7.10	6.20	6.24	6.22
EA	-0.33	0.91	0.92	0.72	0.98	0.60
VIP	7.52	7.56	7.49	6.83	6.86	6.85
VEA	-0.31	-0.53	-0.23	-0.15	-0.05	-0.14
VEAE	-6.41	-6.38	-6.28	-5.55	-5.68	-5.51
VEDE	-1.02	-3.71	-3.63	-1.48	-1.65	-1.50
NRE1	0.59	0.51	0.39	0.64	0.62	0.64
NRE2	0.52	0.68	0.82	0.65	0.57	0.71
NRE3	0.02	1.44	1.15	0.87	1.03	0.74
NRE4	1.35	2.81	2.71	0.76	0.68	0.90
GAP	6.62	7.96	8.02	6.92	7.22	6.82
TD-DFT M06-2X/6-31++G** in aqueous phase						
S1	4.33	4.30	4.28	4.82	4.83	4.81
S2	5.06	4.98	4.97	4.87	4.86	4.87
S3	5.07	5.03	5.04	4.95	4.94	4.95
T1	3.97	3.96	3.96	3.70	3.70	3.70
T2	3.99	3.98	3.98	3.75	3.76	3.75
T3	4.18	4.17	4.16	3.81	3.84	3.81
HOMO	-7.51	-7.50	-7.52	-7.24	-7.22	-7.24
LUMO	-0.21	-0.19	-0.20	-0.54	-0.54	-0.54
GAP	7.30	7.32	7.32	6.70	6.68	6.69

initial radical cation conversion to a neutral molecule, was noted for the phosphate compound, with those for [S_P] and [R_P] d[G_{PS}G] being lower by 0.13eV and 0.03eV (**Table 2**), respectively. Nuclear relaxation energies (**Table 2**), describing the energies necessary for structural changes after electron loss (NRE1) or acceptation (NRE2), followed the orders:
a) NRE1: d[G_{PO}G]>[R_P] d[G_{PS}G]>[S_P] d[G_{PS}G];
b) NRE2: [S_P] d[G_{PS}G]>[R_P] d[G_{PS}G]>d[G_{PO}G].

The above data, HOMO and spin and charge distribution, as well as the results of structural analysis, show that a phosphorothioate linkage can play a role (perhaps a moderate one) during the "hole" migration through the *ss*-DNA. On the contrary, the PT linkage in *ds*-DNA should not play any role in the hole migration process. This conclusion is based on the similarity of AIP, VIP, VEAE, and NRE1 values assigned for the investigated molecules (**Table 2**). Only for NRE2 the differences as low as 0.08eV and 0.06eV were found between d[G_{PO}G]*d[C_{PO}C] and [S_P] and [R_P] d[G_{PS}G]*d[C_{PO}C], respectively. These data are in good agreement with the results of structural analyses, and HOMO and spin and charge distribution, which showed remarkable similarity between double-stranded natural and phosphorothioate oligonucleotides.

Electron Affinity

The electron affinity (EA) of a given system characterizes its electron "trapping" properties **[33].** The adiabatic electron affinity (AEA) is defined as the energy difference between the ground and anionic state of a molecule, and it adopts a positive value for a stable anion. Therefore, the assessment of phosphorothioate linkage influence on oligonucleotide's EAs was important for the electron transfer process through single and double-stranded DNA. The anion may be of a covalent type, in which an extra electron enters LUMO, or of a dipole-bound type, where the electron is bound by the dipole field of a neutral molecule, without influencing its structure **[34].** (The schematic electron migration process is depicted in **Figure 5**.)

The vertical electron affinity (VEA) determines the energy necessary for an immediate electron removal from or fast attachment by a molecule. For all analyzed molecules, VEA adopt negative values (see **Table 2**) and for d[G_{PX}G] (X=O or S) they increase (become less negative) in the order: [R_P]<PO<[S_P]. They are also more negative than those assigned for d[G_{PX}G]*d[C_{PO}C] (X=O or S), which increase in the order: PO<[S_P]<[R_P]. The vertical energy found for the R_P diastereomer of d[G_{PS}G]*d[C_{PO}C] is close to zero (-0.05 eV, the least negative value), while for R_P d[G_{PS}G] it is the most negative of all investigated *ss*-dinucleotides (**Table 2**).

Analysis of AEA (which corresponds to the relaxed attaching energy **[26]** gave a negative value for d[G_{PO}G]. It is in good agreement with radical anion spatial geometry, which disallows the stacking interaction, otherwise present in a neutral form. Moreover, SOMO was localized near the phosphate group between two sugar moieties, prone to the dipole-bond character. It was confirmed by a dipole moment value of 18.41[D].

The presence of the phosphorotioate bond in d[G_{PS}G] system protects the stacking interaction and results in positive AEA value, which for both R_P and S_P diastereomers, were virtually the same (**Table 2**). Due to the localization of SOMO and low dipole moment value (**Table 3SM** and **Figure 9SM**), it can be postulated that the phosphorothioate radical anions show a covalent-bond character.

The complementary d[C_{PO}C] brings significant consequences to the double-stranded systems. The AEA energies adopt positive values decreasing in the order [R_P] d[G_{PS}G]*d[C_{PO}C]>d[G_{PO}G]*d[C_{PO}C]>[S_P] d[G_{PS}G]*d[C_{PO}C]. The spin analysis showed that the excess electron is mainly located on the 3'-site cytidine (**Figure 11SM**). Moreover the dipole moment value points to a covalent anion character, rather than to a dipole (**Table 4SM**). This clearly indicates that, due to the rigidity of *ds*-DNA, the attached electron does not change significantly the spatial geometry of the double-helix.

In the context of electron migration through oligonucleotide strands, the relaxation energy is crucial for the electron transition from one nucleobase/phosphate group to another. For this process the value of nuclear relaxation energy (NRE) is a good predictor. First, NRE3 shows the energy necessary, after electron attachment, for compensation of the structural changes. For d[G_{PO}G] this value was as low as 0.02eV, so the electronic structure of the molecule was not damaged. For [R_P] and [S_P] d[G_{PS}G] the corresponding values were significantly higher. It could be expected, because the P-S bond in phosphorothioate diesters is elongated. For the same reasons, the NRE4 energies, required for geometry relaxation after electron loss, decrease in the order: [R_P] d[G_{PS}G]>[S_P] d[G_{PS}G]>d[G_{PO}G].

For the investigated double-stranded d[G_{PX}G]*d[C_{PO}C] (X=O or S), the nuclear relaxation energies were found at the same level, as shown in **Table 2**. The orders of NER 3 and NER4 were: [R_P]>PO>[S_P] and [S_P]>PO>[R_P], respectively. However, the average difference between phosphate and phosphorothioate was at the level of ±0.13eV.

It has been clearly shown that the trapped electron is more strongly bound by *ds*-DNA than by a *ss*-oligonucleotide. On the other hand, a single DNA strand captures an electron more effectively than a double-helix. This is because in *ss*-DNA, an electron directly attaches to the phosphate or phosphorothioate group, which is more easily available than that in *ds*-DNA, where an intermolecular electron migration to the pirymidine moiety is necessary.

The energy gap (GAP) between a radical anion and a cation well characterizes the stability of a given radical. In these studies, GAP found for d[G_{PO}G] was by ~1.4eV lower than for [R_P] and [S_P] d[G_{PS}G]. Therefore, the phosphate analog should form a more stable radical than the phosphorothioates, and this result goes along with the structural analysis. On the other hand, the GAP values for *ds*-DNA were at the same level for all the discussed molecules, independently of the presence of sulfur. So, one may conclude that in double-stranded oligonucleotides, the phosphorothioate internucleotide bond should not play any significant role in the electron attachment process.

For the assessment of excitation energy, the TD-DFT methodology at the M06-2X/6-31++G** level of theory in an aqueous phase was used. For all molecules, the single point calculations showed the preferential formation of the triplet state. Moreover, within a given family of oligomers (*ss* or *ds*) almost the same energies for HOMO, LUMO and GAP were found (**Table 2**). Because the LUMO energies for the d[G_{PX}G] system were less negative than for d[G_{PX}G]*d[C_{PO}C] (X=O or S), it can be expected that the single-strand oligomers in the aqueous phase will form corresponding radical anions more effectively than the double-stranded ones. On the contrary, the GAP energies for *ds*-DNA were found to be lower than for *ss*-oligonucleotide, which within the double-helix should lead to the formation of more stable radical anions. These theoretical data are in good agreement with experimental data presented by Ray *et al.* **[31]**.

Conclusions

The presence of phosphorothioate bond in the model double-stranded PS-DNAs did not affect significantly the spatial geometry of their neutral radical anion and cation forms, as compared with the phosphate congener. Opposite to that, in the case of *ss*-DNA, its higher flexibility gave rise to the fluctuation of geometries. Moreover, the capture of an electron leads to the radical anion forms possessing the P-S bond broken, yet with prevented possibility of stacking interaction between the adjacent bases. In the radical anion form of the d[G_{PO}G] phosphate dinucleotide only linearization of the structure was observed (**Figures 4, 3**).

Based on the spin density distribution analysis it can be postulated that the d[G_{PO}G] radical anion has a dipole valence character, while those of phosphorothioate analogs have a covalent character. This indicates that the desulfurization process can be initiated by elongation of the P-S bond in the presence of an extra electron.

Analysis of the electronic parameters did not show any significant differences between phosphate, *ss*- and *ds*-phosphorothioate oligonucleotides (**Table 2**). Therefore, PT should not disturb the charge "hole" migration through a double-helix or a single-strand of DNA. This conclusion can be supported by a comprehensive structural analysis. However, the electron migration process through a *ss*-phosphorothioate oligonucleotide may be either slowed down or (in extreme cases) quenched. This is due to the extra electron loss during the desulfurization process.

It is important to mention that for all phosphorothioate and phosphate nucleotides the triplet excitation state was found to be preferred (**Table 2**). Moreover, in the aqueous phase, LUMO energies for d[G_{PX}G] were lower than for d[G_{PX}G]*d[C_{PO}C] (X=O or S). Therefore, it can be expected that a single-strand oligomer will form a radical anion more effectively than a double-stranded one. Conversely, GAP for *ds*-DNA was found lower than for *ss*-oligonucleotide, which should lead to the formation of more stable radical anion within the double-helix.

Experimental

Computation Methodology of Quantum Mechanics Study

All the calculations (geometry optimization) were performed by the density functional theory (DFT) using the M06-2X functional **[35]**. M06-2X is a hybrid meta-generalized gradient approximation (GGA) exchange functional (DFT method) developed by Truhlar, who recommended the augmented

polarized valence double-ζ basis set 6-31+G(d,p) for this functional [36]. The characterization of the singlet and triplet excited states the single point calculation at the M06-2X/6-31++G(d,p) level of theory in athe queous phase was performed using time-dependent DFT (TD-DFT) methodology **[37]**.

The appropriate adiabatic electron affinities (AEA) were obtained as a difference between the energies of the appropriate neutral ($E_{Neutral}$) and anion (E_{Anion}) forms at their optimized geometries AEA = $E_{Neutral}(r_e,0) - E_{Anion}(r_e,^-)$ **[38]**. In this study, the electron affinity is defined as the energy released when the electron is added to a neutral molecule **[39]**.

The vertical electron affinities (VEA) were obtained as a difference between the energies of the appropriate neutral ($E_{Neutral}$) and anion (E_{Anion}) forms at optimized neutral geometries VEA = $E_{Neutral}(r_e,0) - E_{Anion}(r_e,0)$ **[38]**.

The vertical electron detachment energies (VEDE) were obtained as a difference between the energies of the appropriate neutral ($E_{Neutral}$) and anion (E_{Anion}) forms at optimized anion geometries VEDE = $E_{Anion}(r_e,^-) - E_{Neutral}(r_e,^-)$ **[40]**.

From the definition, the ionization potential is the amount of energy required to remove an electron from a molecule. The suitable adiabatic ionization potential (AIP) was obtained as the difference between the energies of the appropriate cationic (E_{Cation}) and neutral ($E_{Neutral}$) forms at their optimized geometries AIP = $E_{Cation}(r_e,^+) - E_{neutral}(r_e,0)$ **[41]**.

The vertical ionization potential VIP was obtained as the difference between the energies of the appropriate cation (E_{Cation}) and neutral ($E_{Neutral}$) forms at optimized neutral geometries VIP = $E_{Cation}(r_e,0) – E_{Neutral}(r_e,0)$ **[41]**.

The vertical electron affinity of cations, in this article noted as vertical electron attachment energy (VEAE), was obtained as the difference between the energies of the appropriate neutral ($E_{Neutral}$) and cation (E_{Cation}) forms at optimized cation geometries VEAE = $E_{Cation}(r_e,^+) - E_{Neutral}(r_e,^+)$ **[40]**.

All calculations were performed in the gaseous phase on Gaussian 09 (revision A.02) software package **[42]**. The visualization of all the structures, as well as the creation of suitable *.pdb files was performed using DS Visualizer software **[43]**. The three-dimensional structural analyses of the mentioned *ss*- and *ds*-DNAs, based on a standard reference frame, were obtained by a 3DNA software package using the web based interface w3DNA (web 3DNA) **[44]**.

Acknowledgements

This work was supported by the Polish Ministry of Science and Higher Education (**NN 405 615 838**), Medical University of Lodz (**503-31-002**) for which the author is grateful.

Notes

[a] Food Science Department, Medical University of Lodz, ul. Muszynskiego 1, 90-151 Lodz, Poland. e-mail: Bolek.Karwowski@wp.pl

†Electronic Supplementary Information (ESI) available: [Tables of structural parameters and charge distribution; Graphical visualisation of HOMO, LUMO, spin density distribution; Graphical representation of structural comparative studies]. See DOI: 10.1039/b000000x/

References

1. X. Zhao, Z. deng, J.L. Firmi, D.A. Hopwood, T. Kieser, *Nucleic Acid. Res.,* 1988, **16**, 4341
2. a) A. Boybek, T.D. Ray, M.C. Evans, P.J. Dyson, *Nucleic Acid. Res.*, 1988, **26**, 3364, b) X. Zhou, X. He, J. Ling, A. Li, T. Kieser, J.D. Helmann, Z. Deng, *Mol. Microbol.*, 2005, **57**, 1428
3. L. Wang, S. Chen, T. Xu, K. Taghizadeh, J.S. Wishnok, X. Zhou, D. You, Z. Deng, P.C. Dedon, *Nat. Chem. Biol.,* 2007, **3**, 709
4. P.J. Furdon, Z. Domanski, R. Kole, *Nucleic Acid. Res.* 1989, **17**, 9193
5. S. Spitzer, F. Eckstein, *Nucleic Acid. Res.,* 1988, **16**, 11691
6. F. Eckstein, *Antisense Nucleic Acid Drug Dev*., 2000, **10**, 117
7. P.M. Burgers, F. Eckstein, *J. Biol. Chem.*, 1979, **254**, 6889
8. S. Chen, L. Wang, Z. Dend, *Protein&Cell*, 2010, **1**, 14
9. W. J. Stec, A. Grajkowski, M. Koziołkiewicz, B. Uznański, *Nucleic Acids Res*., 1991, **19**, 5883
10. P. Guga, *Curr. Top. Med. Chem*., 2007, **7**, 695
11. C.M. Perry, J.A. Barman Balfour, *Drug*, 1999, **3**, 375
12. X. Xie, J. Liang, T. Pu, F.Xu, F. Yao, Y. Yang, Y-L. Zhao, D. You, X. Zhou, Z. Deng, Z. Wang, *Nucleic Acid. Res.,* 2012, **40**, 9115
13. a) C. Von Sontag, *Free Radical Induced DNA damage and its Repair. A Chemical Perspective*. Springer-Verlag Berlin Heidelberg, 2006, b) M.D. Greenberg, *Radical and Radical Ion Reactivity in Nucleic Acid Chemistry*. John Wiley & Sons, 2009
14. H.J. Helbock, K.B. Beckman, B.N. Ames, *Methods Enzymol.*, 1999, **300**, 156
15. S. Kanvah, G.B. Schusre, Pure Appl. Chem., 2006, **78**, 2297
16. L. Wu, D.E. White, C. Ye, F.G. Vogt, G.J. Terfloth, H. Matsuhashi, J. Mass. Spectrom., 2012, **47**, 836
17. A. Adhikary, A. Kumar, B.J. Palmer, A.D. Todd, M.D. Sevilla, J. Am. Chem. Soc., 2013, **135**, 12827
18. A. Alt, K. Lammens, C. Chiocchini, A. Lammens, J.C. Pieck, D. Kuch, K.P. Hopfner,T. Carell, Science, 2007, 318, 967
19. a) W.K. Olson, M. Bansal, S.K. Burley, R.E. Dickerson, M.Gerstein, S.C. Harvey, U. Heinemann, X-J. Lu, S. Neidle, Z. Shakked,H. Sklenar, M. Suzuki, C-S Tung, E. Westhof, C. Wolberger, H.M. Berman, J. Mol. Biol., 2001, **313**, 229, b) L. Chen, X-L. Wang, T. Shi, T. Wu, Z. Deng, Y-L. Zhao, J. Phys. Chem. B, 2015, **119**, 474
20. A.V. Marenich, S.V. Jerome, Ch.J. Cramer, D.G. Truhlar, J. Chem. Theory Comput., 2012, 8, 527 (and citations ibid)
21. A. Kumar, M.D. Sevilla, S. Suhai, *J. Phys. Chem.B,* 2008, **112**, 5189
22. J. Gu,Y. Xie, H.F. Schaefer III, *Chem. Phys. Lett.*, 2009, **437**, 213
23. X. Bao, J. Wang, J. Gu, J. Leszczynski, *PNAS*, 2006, **103**, 5658
24. a) F. Plasser, H. Lischka *Photochem. & Photobiol. Sci.,* 2013, **12**, 1440, b) Y. Paukku, G. Hill, J. Phys. Chem. A, 2011, **115**, 4804, c) J. Gu, J. Wang, J. Leszczyski, Nucleic Acids Res., 2010, **38**, 5280, d)A. Kumar, M.D. Sevilla, *J. Phys. Chem. B,* 2009, **113**, 11359
25. Y-C. Zhang, J. Liang, P. Lian, Y. Han, Y. Chen, L. Bai, Z. Wang, J. Liang, Z. eng, Y-L. Zhao, *J. Phys. Chem. B*, 2012, **116**, 10639
26. A. Kumar, M.D. Sewilla, *J. Phys. Chem. B*, 2011, **115**, 4990
27. a) X. Li, M.D. Sevilla, L. Sanche, *J. Am. Chem. Soc*., 2003, **125**, 13668, b) B.T. Karwowski, *Cent. Eur. J. Chem.*, 2013, 11, 1079
28. M.D. Sevilla, D. Becker, M. Yan, S.R. Summerfield, *J. Phys. Chem.*, 1991, **95**, 3409
29. H. Sugiyama, I. Saito, *J. Am. Chem. Soc.*, 1996, **118**, 7063

30. a) G.B. Shuster, U. Landman, Top Curr. Chem. 2004,. **236**, 139, b) J.C. Genereux, J.K. Barton, Chem. Rev., 2010 **110**, 1642, c) B. Giese, J. Amaudurut, A-K. Kohler, M. Sporman, S. Wessely, Nature, 2001, **412**, 318, d) B. Giese, Acc. Chem. Res., 2000, **33**, 631
31. S.G.. Ray, S.S. Daube, R. Naaman, *PNAS*, 2005, **102**, 15
32. D. Khanduri, A. Adhikary, M.D. Sevilla, *Radical and Radical Ion Reactivity in Nucleic Acid Chemistry*, John Wiley Sons, Inc., New Jersey, 2009, 1
33. J.C. Rienstra-Kiracofe, G.S. Tschumper, H.F. Schaefer III, S. Nandi, B. Ellison, *Chem. Rev*., 2002, **102**, 231
34. a) N.A. Oyler, L. Adamowicz, *J. Phys. Chem.,* 1993, **97**, 11122, b) P. Sarmah, R.C. Deka, *Mol. Simulat*., 2008, **34**, 879
35. a) Y. Zhao, J. Pu, B.J. Lynch, D.G. Truhlar *PCCP*, 2004, **6**, 673, b) Y. Zhao, D.G. Truhlar, *J. Phys. Chem., A,*2005, **109**, 5656
36. W.J. Hehre, L. Radom, P. Schleyer, R.J.A. Pople *Ab Initio Molecular Orbital* Theory; Wiley, New York, 1986, pp. 63-101
37. E. Rugne, E.K.U. Gross, *Phys. Rev. Lett.*1984, **52**, 997
38. J.C. Rienstra-Kiracofe, G.S. Tschumper, H.F. Schaefer, III, S. Nandi and B. Ellison, *Chem. Rev.*, 2002, **102**, 231
39. Ch-G Zhan, J.A. Nichols, D.A. Dixon, *J. Phys. Chem. A* 2003, **107**, 4184
40. X. Li, Z. Cai and M.D. Sevilla, *J. Phys. Chem. A.,* 2002, **106**, 9345
41. J.B. Foresman, A Frisch, *Exploring Chemistry with Electronic Structure Methods*; Gaussian, Inc. Pittsburgh, PA, (2nd edition), 1996, pp. 141-160.
42. M.J. Frisch, G.W. Trucks, H.B. Schlegel, G.E. Scuseria, M.A. Robb, J. R. Cheeseman, G. Scalmani, V. Barone, B. Mennucci, G.A. Petersson, H. Nakatsuji, M. Caricato, X. Li, H.P. Hratchian, A.F. Izmaylov, J. Bloino, G. Zheng, J.L. Sonnenberg, M. Hada, M. Ehara, K. Toyota, R. Fukuda, J. Hasegawa, M. Ishida, T. Nakajima, Y. Honda, O. Kitao, H. Nakai, T. Vreven, J. A. Montgomery, Jr., J.E Peralta,., F. Ogliaro, M. Bearpark, J.J. Heyd, E. Brothers, K.N. Kudin, V.N. Staroverov, R. Kobayashi, J. Normand, K. Raghavachari, A. Rendell, J.C. Burant, S.S. Iyengar, J. Tomasi, M. Cossi, N. RegaJ.M. , Millam, M. Klene, J.E. Knox, J.B. Cross, V. Bakken, C. Adamo, J. Jaramillo, R. Gomperts, R.E. Stratmann, O. Yazyev, A.J. Austin, R. Cammi, C. Pomelli, J.W. Ochterski, R.L. Martin, K. Morokuma, V.G. Zakrzewski, G.A. Voth, P. Salvador, J.J. Dannenberg, S. Dapprich, A.D. Daniels, O. Farkas, J.B. Foresman, J.V. Ortiz, J. Cioslowski and D.J. Fox (2009) Gaussian 09, Revision A.02, Gaussian, Inc., Wallingford CT.
43. Accelrys DS Visualizer v2.0.1.7347, Accelrys Software Inc. Copyright © 2005–2007 (Freeware version).
44. G. Zheng, X.-J. Lu and W. K. Olson, *Nucleic Acids Res*., 2009, **37** (Web Server issue), W240–W246, b) X.-J. Lu, W. K. Olson, *Nucleic Acids Res*., 2003, **31**, 5108, c) X.-J. Lu, W. K. Olson, *Nat. Protoc*., 2008, **3**, 1213

